Doped Sr_2FeIrO_6 – phase separation and a $J_{eff} \neq 0$ state for Ir^{5+}

Jacob E. Page, Craig V. Topping, Alex Scrimshire, Paul A. Bingham, Stephen J. Blundell and Michael A. Hayward *.

Supporting Information

Table of Contents

1. Structural Characterization of Sr_2FeIrO_6

Atom	x	y	z	Fraction	U_{iso} (Å^2)
Sr	0.499(2)	0.499(2)	0.250(1)	1	0.0051(4)
Fe/Ir(1)	0	½	0	0.91(1)/0.09(1)	0.0032(2)
Ir/Fe(2)	½	0	0	0.91(1)/0.09(1)	0.0032(2)
O(1)	0.259(3)	0.260(2)	0.984(2)	1	0.0010(1)
O(2)	0.247(3)	0.755(3)	0.026(2)	1	0.0010(1)
O(3)	0.501(3)	0.038(3)	0.249(2)	1	0.0010(1)
Sr_2FeIrO_6 – space group $I\bar{1}$ (#2) Formula weight : 519.30 g mol^{-1}, Z = 2 a = 5.5519(2) Å, b = 5.5779(2) Å, c = 7.8445(2) Å, α = 90.01(1)º, β = 90.04(1) º, γ = 90.10(1)º					
Radiation source: Synchrotron X-ray, λ = 0.82626(1) Temperature: 298 K χ^2 = 14.13; *wRp*= 2.55 %; *Rp* = 1.70 %.					

Table S1. Structural parameters from the refinement of Sr_2FeIrO_6 against synchrotron X-ray powder diffraction data.

Cation	Anion	length (Å)
Fe(1)	O(1)	1.970(17)
Fe(1)	O(2)	1.984(19)
Fe(1)	O(3)	1.980(16)
Ir(2)	O(1)	1.979(17)
Ir(2)	O(2)	1.969(19)
Ir(2)	O(3)	1.965(16)

Table S2. Selected bond lengths from the refined structure of Sr_2FeIrO_6

2. Structural Characterization of $La_{0.05}Sr_{1.95}FeIrO_6$

Atom	x	y	z	Fraction	U_{iso} (Å^2)
La/Sr	0.499(1)	0.499(1)	0.250(1)	0.025/0.975	0.0070(3)
Fe/Ir(1)	0	½	0	0.91(1)/0.09(1)	0.0055(2)
Ir/Fe(2)	½	0	0	0.91(1)/0.09(1)	0.0055(2)
O(1)	0.258(1)	0.259(1)	0.984(1)	1	0.0049(2)
O(2)	0.247(1)	0.756(1)	0.025(1)	1	0.0079(2)
O(3)	0.502(1)	0.036(1)	0.250(1)	1	0.0036(1)
$La_{0.05}Sr_{1.95}FeIrO_6$ – space group $I\bar{1}$ (#2) Formula weight : 521.87 g mol^{-1}, Z = 2 Weight fraction: 44.3(9)% *a* = 5.5497(1) Å, *b* = 5.5781(1) Å, *c* = 7.8463(1) Å, α = 89.99(1)º, β = 90.06(1) º, γ = 90.07(2)º					
Atom	x	y	z	Fraction	U_{iso} (Å^2)
La/Sr	0.996(1)	0.000(1)	0.266(1)	0.025/0.975	0.0050(1)
Fe/Ir(1)	½	0	½	0.84(1)/0.16(1)	0.0063(2)
Ir/Fe(2)	½	0	0	0.84(1)/0.16(1)	0.0063(2)
O(1)	0.227(1)	0.224(1)	0.020(1)	1	0.0104(2)
O(2)	0.246(1)	0.758(1)	0.013(1)	1	0.0061(2)
O(3)	0.970(1)	0.502(2)	0.251(2)	1	0.0083(2)
$La_{0.05}Sr_{1.95}FeIrO_6$ – space group $P2_1/n$ (#14) Formula weight : 521.87 g mol^{-1}, Z = 2 Weight fraction: 55.7(9)% *a* = 5.5515(1) Å, *b* = 5.5810(1) Å, *c* = 7.8462(1) Å, β = 90.08(1) º					
Radiation source: Time-of-flight neutron diffraction Temperature: 298 K χ^2 = 50.23; *wRp*= 5.91 %; *Rp* = 4.06 %.					

Table S3. Structural parameters from the 2-phase refinement of $La_{0.05}Sr_{1.95}FeIrO_6$ against neutron powder diffraction data collected at 250 K

$I\bar{1}$			$P2_1/n$		
Cation	Anion	length (Å)	Cation	Anion	length (Å)
Fe(1)	O(1)	1.969(20)	Fe(1)	O(1)	1.996(6)
Fe(1)	O(2)	1.988(21)	Fe(1)	O(2)	1.987(6)
Fe(1)	O(3)	1.972(8)	Fe(1)	O(3)	1.977(16)
Ir(2)	O(1)	1.978(20)	Ir(2)	O(1)	1.971(6)
Ir(2)	O(2)	1.964(20)	Ir(2)	O(2)	1.955(6)
Ir(2)	O(3)	1.972(8)	Ir(2)	O(3)	1.961(16)

Table S4. Selected bond lengths from the 2-phase refinement of $La_{0.05}Sr_{1.95}FeIrO_6$ against neutron powder diffraction data collected at 250 K.

3. Magnetic Characterization of $La_{0.05}Sr_{1.95}FeIrO_6$

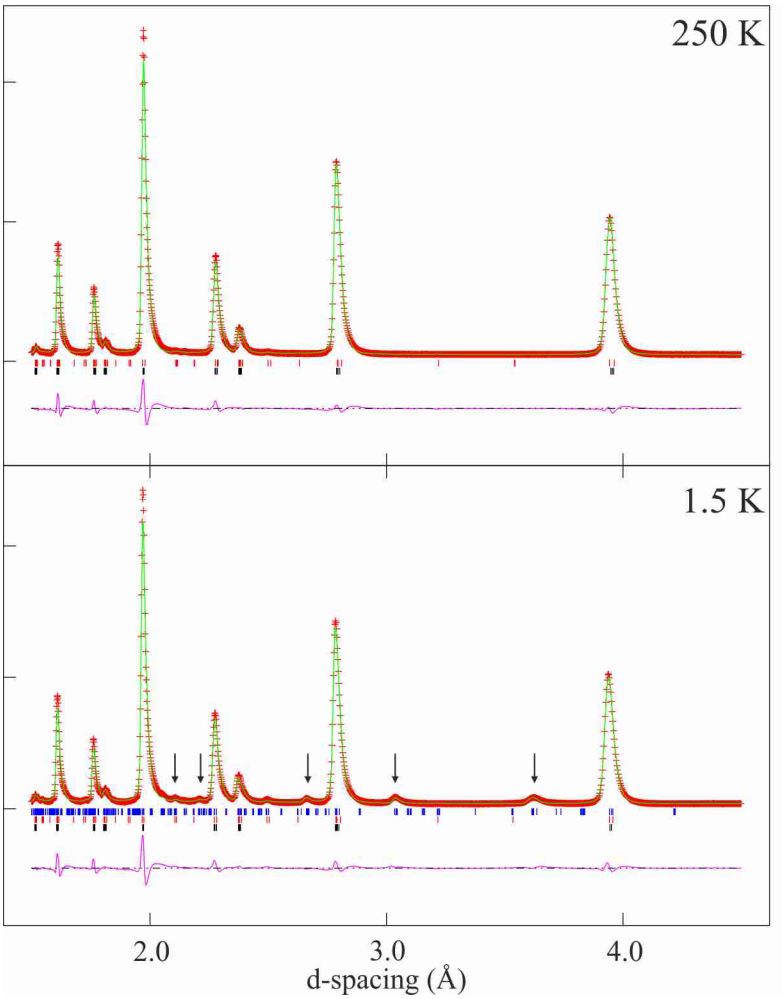

Figure S1 Observed calculated and difference plots from the structural and magnetic refinement of $La_{0.05}Sr_{1.95}FeIrO_6$ against neutron powder diffraction data collected at 1.5 K (bottom), compared to a structure only refinement against the equivalent data collected 250 K. Arrows mark the most obvious additional magnetic reflections. Blue, red and black tick marks correspond to allowed peak positions for the magnetic, $P2_1/n$ and $I\bar{1}$ phases respectively.

Atom	x	y	z	Fraction	U_{iso} (Å^2)
La/Sr	0.499(1)	0.499(1)	0.250(1)	0.025/0.975	0.0068(3)
Fe/Ir(1)	0	½	0	0.91/0.09	0.0054(2)
Ir/Fe(2)	½	0	0	0.91/0.09	0.0054(2)
O(1)	0.258(1)	0.259(1)	0.984(1)	1	0.0043(2)
O(2)	0.247(1)	0.756(1)	0.025(1)	1	0.0071(2)
O(3)	0.502(1)	0.036(1)	0.250(1)	1	0.0034(1)
$La_{0.05}Sr_{1.95}FeIrO_6$ – space group $I\bar{1}$ (#2) Formula weight : 521.87 g mol^{-1}, Z = 2 Weight fraction: 44.3% *a* = 5.5481(1) Å, *b* = 5.5765(1) Å, *c* = 7.8452(1) Å, α = 89.99(1)º, β = 90.07(1) º, γ = 90.06(2)º					
Atom	x	y	z	Fraction	U_{iso} (Å^2)
La/Sr	0.997(1)	0.000(1)	0.264(1)	0.025/0.975	0.0049(1)
Fe/Ir(1)	½	0	½	0.84/0.16	0.0061(2)
Ir/Fe(2)	½	0	0	0.84/0.16	0.0061(2)
O(1)	0.227(1)	0.224(1)	0.020(1)	1	0.0098(2)
O(2)	0.246(1)	0.758(1)	0.013(1)	1	0.0058(2)
O(3)	0.970(1)	0.502(2)	0.251(2)	1	0.0081(2)
$La_{0.05}Sr_{1.95}FeIrO_6$ – space group $P2_1/n$ (#14) Formula weight : 521.87 g mol^{-1}, Z = 2 Weight fraction: 55.7(9)% *a* = 5.5512(1) Å, *b* = 5.5808(1) Å, *c* = 7.8458(1) Å, β = 90.08(1) º					
Radiation source: Time-of-flight neutron diffraction Temperature: 298 K χ^2 = 59.85; *wRp*= 6.54 %; *Rp* = 5.14 %.					

Table S5. Structural parameters from the 2-phase refinement of $La_{0.05}Sr_{1.95}FeIrO_6$ against neutron powder diffraction data at 1.5 K

Atom	x	y	x	M_Z
Fe(1)	½	0	0	2.92(2)
Fe(2)	½	½	0	-2.92(2)
Fe(3)	0	¼	¼	2.92(2)
Fe(4)	0	¾	¼	-2.92(2)
Fe(5)	½	0	½	-2.92(2)
Fe(6)	½	½	½	2.92(2)
Fe(7)	0	¼	¾	-2.92(2)
Fe(8)	0	¾	¾	2.92(2)

Table S6. Parameters from the magnetic refinement of $La_{0.05}Sr_{1.95}FeIrO_6$ against neutron powder diffraction data at 1.5 K

Temperature (K)	Phase Fraction $I\bar{1}$	Phase Fraction $P2_1/n$
1.5	43.8(9)	56.2(9)
25	44.1(9)	55.9(9)
50	44.0(9)	56.0(9)
100	43.9(8)	56.1(8)
125	44.2(9)	55.8(9)
150	43.3(9)	56.7(9)
200	43.6(8)	56.4(9)
250	44.3(9)	55.7(9)

Table S7. Phase fractions from the structural refinement of $La_{0.05}Sr_{1.95}FeIrO_6$ against neutron powder diffraction data.

4. Structural Characterization of $Sr_{2-x}A_xFeIrO_6$ and $Sr_2Fe_{0.05}Ga_{0.05}IrO_6$

	Synchrotron X-ray		
Space Group	χ^2	wRp (%)	Rp (%)
$I\bar{1}$ (#2)	5.189	1.70	1.24
I2/m (#12)	6.439	1.89	1.33
$P2_1/n$ (#14)	6.365	1.88	1.33
$I\bar{1}$ + $P2_1/n$	4.032	1.54	1.14
I2/m + $P2_1/n$	4.742	1.67	1.19

Table S8. Fitting statistics from the structural refinement of $La_{0.025}Sr_{1.975}FeIrO_6$ against synchrotron X-ray powder diffraction data

	Synchrotron X-ray		
Space Group	χ^2	wRp (%)	Rp (%)
$I\bar{1}$ (#2)	18.57	2.58	1.78
I2/m (#12)	22.90	2.87	1.92
$P2_1/n$ (#14)	22.89	2.87	1.92
$I\bar{1}$ + $P2_1/n$	16.45	2.43	1.70
I2/m + $P2_1/n$	17.73	2.53	1.77

Table S9. Fitting statistics from the structural refinement of $Sr_{1.95}Ca_{0.05}FeIrO_6$ against synchrotron X-ray powder diffraction data

	Synchrotron X-ray		
Space Group	χ^2	wRp (%)	Rp (%)
$I\bar{1}$ (#2)	9.389	2.17	1.54
I2/m (#12)	11.15	2.37	1.63
$P2_1/n$ (#14)	11.33	2.39	1.62
$I\bar{1}$ + $P2_1/n$	8.565	2.04	1.49
I2/m + $P2_1/n$	9.011	2.13	1.53

Table S10. Fitting statistics from the structural refinement of $Ba_{0.0185}Ca_{0.0315}Sr_{1.95}FeIrO_6$ against synchrotron X-ray powder diffraction data

	Synchrotron X-ray		
Space Group	χ^2	wRp (%)	Rp (%)
$I\bar{1}$ (#2)	13.00	2.36	1.62
I2/m (#12)	18.72	2.66	1.91
$P2_1/n$ (#14)	19.11	2.68	1.93
$I\bar{1}$ + $P2_1/n$	9.987	2.06	1.47
I2/m + $P2_1/n$	11.06	2.18	1.52

Table S11. Fitting statistics from the structural refinement of $Sr_2Fe_{0.95}Ga_{0.05}$ IrO_6 against synchrotron X-ray powder diffraction data

5. Magnetization-field isotherms from $Sr_{2-x}A_xFe_{1-x}Ga_xIrO_6$ phases

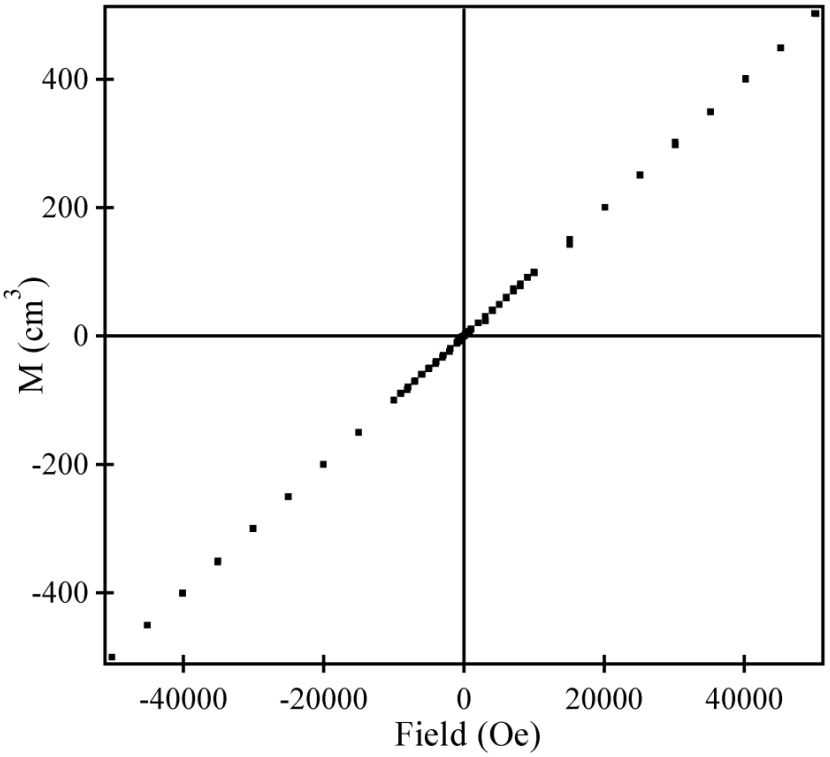

Figure S3. Magnetization-field isotherms collected from Sr_2FeIrO_6 at 5K and 300 K

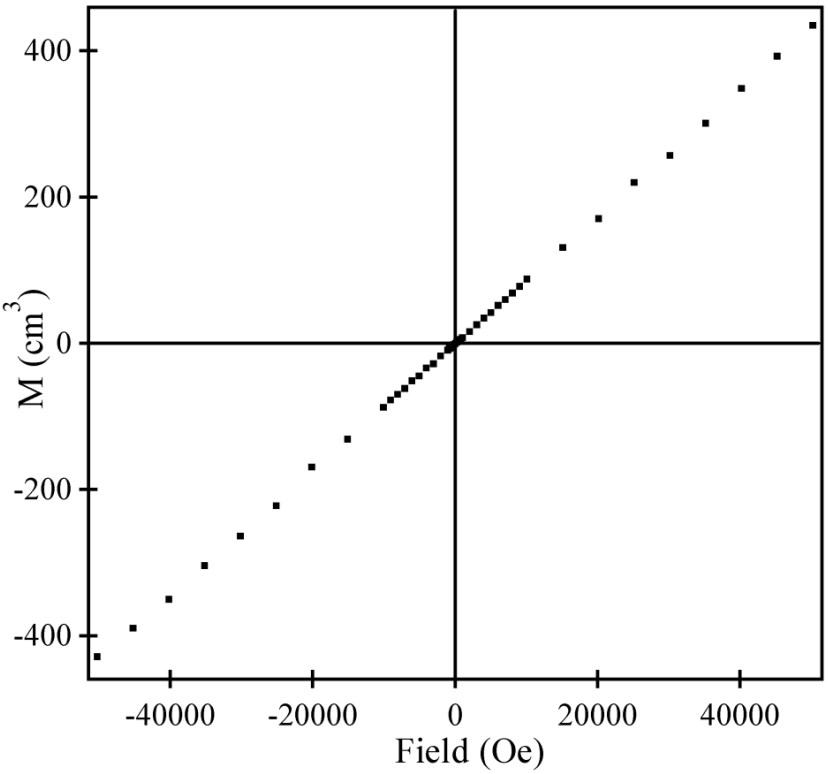

Figure S4. Magnetization-field isotherms collected from $La_{0.05}Sr_{1.95}FeIrO_6$ at 300 K

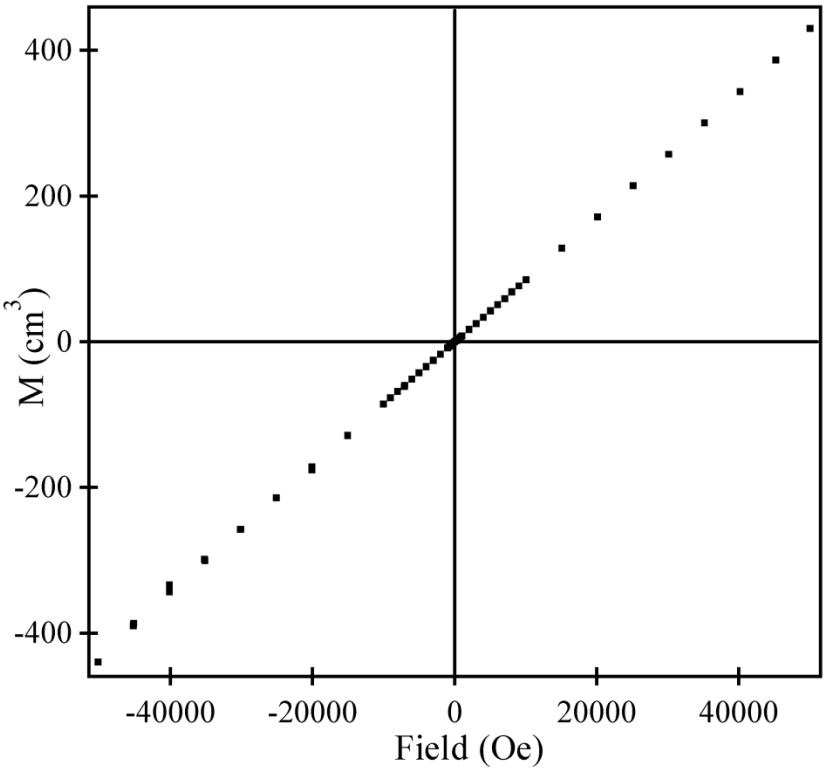

Figure S5. Magnetization-field isotherms collected from $La_{0.025}Sr_{1.975}FeIrO_6$ at 300 K

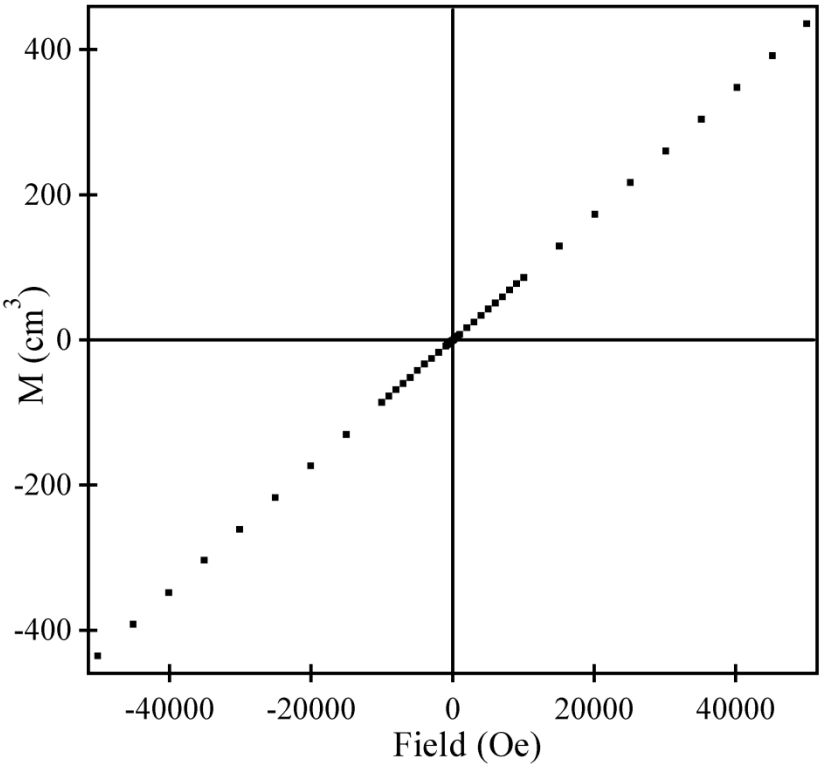

Figure S6. Magnetization-field isotherms collected from $Ca_{0.05}Sr_{1.95}FeIrO_6$ at 300 K

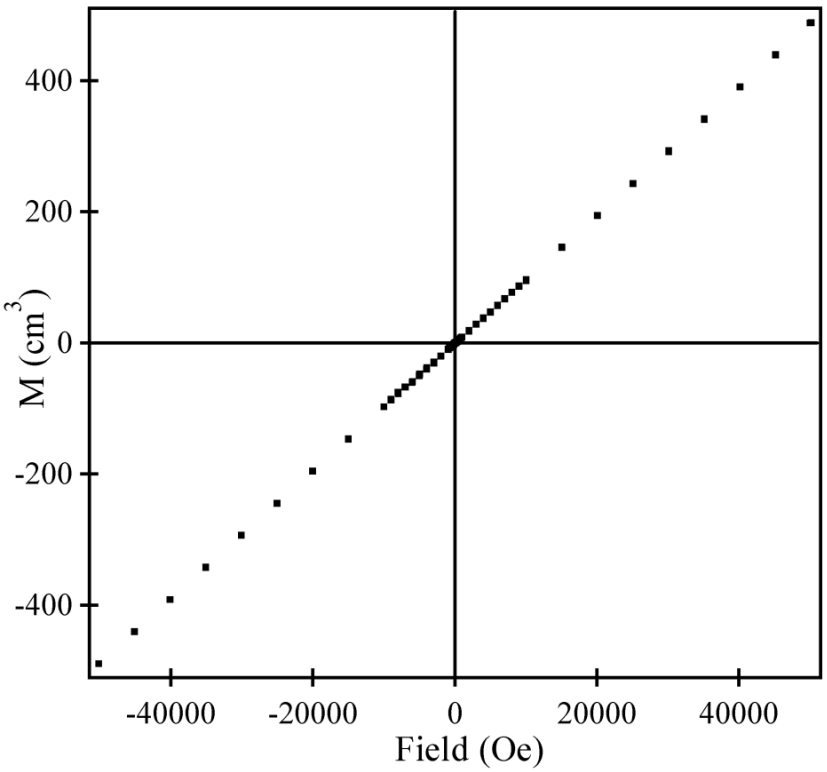

Figure S7. Magnetization-field isotherms collected from $Ba_{0.0185}Ca_{0.0315}Sr_{1.95}FeIrO_6$ at 300 K

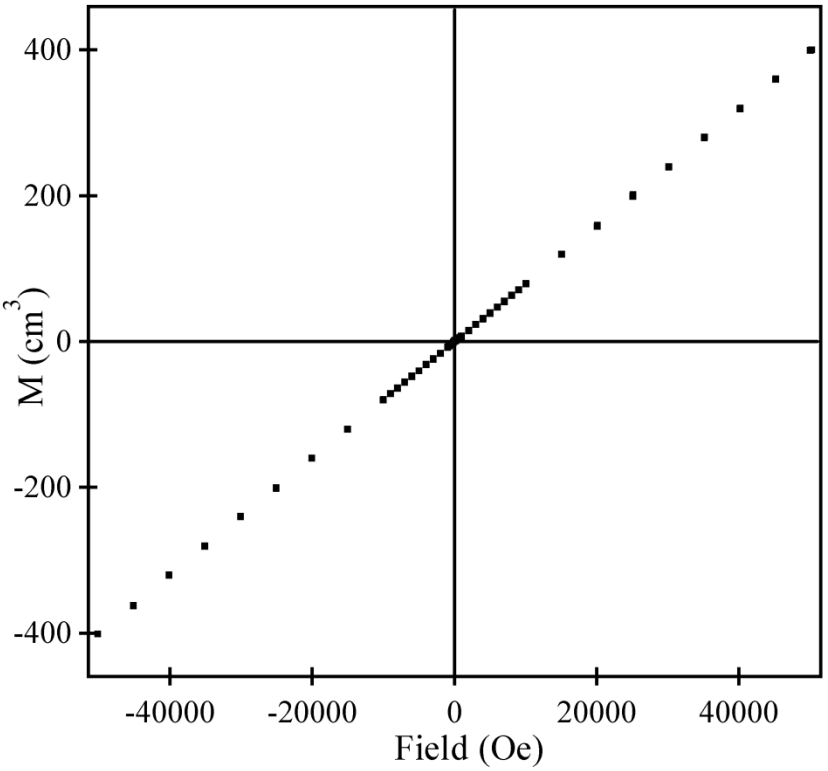

Figure S8. Magnetization-field isotherms collected from $Sr_2Fe_{1.95}Gaa_{0.05}IrO_6$ at 300 K

6. Temperature dependent lattice parameters of $I\bar{1}$ phase of $La_{0.05}Sr_{1.95}FeIrO_6$

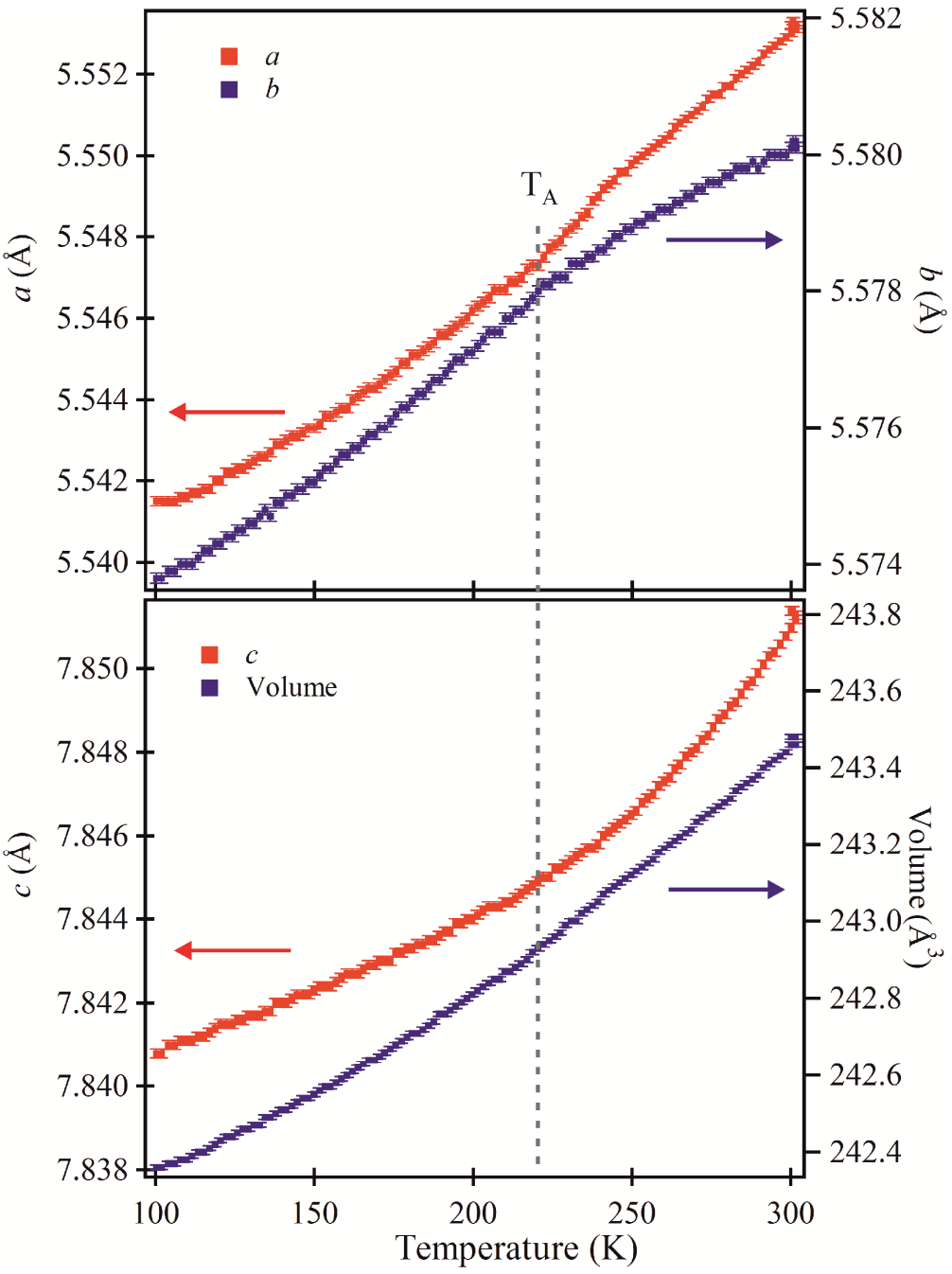

Figure S9. Lattice parameters and cell volume of the $I\bar{1}$ phase of $La_{0.05}Sr_{1.95}FeIrO_6$, obtained from synchrotron X-ray powder diffraction data, plotted as a function of temperature

7. Transport data

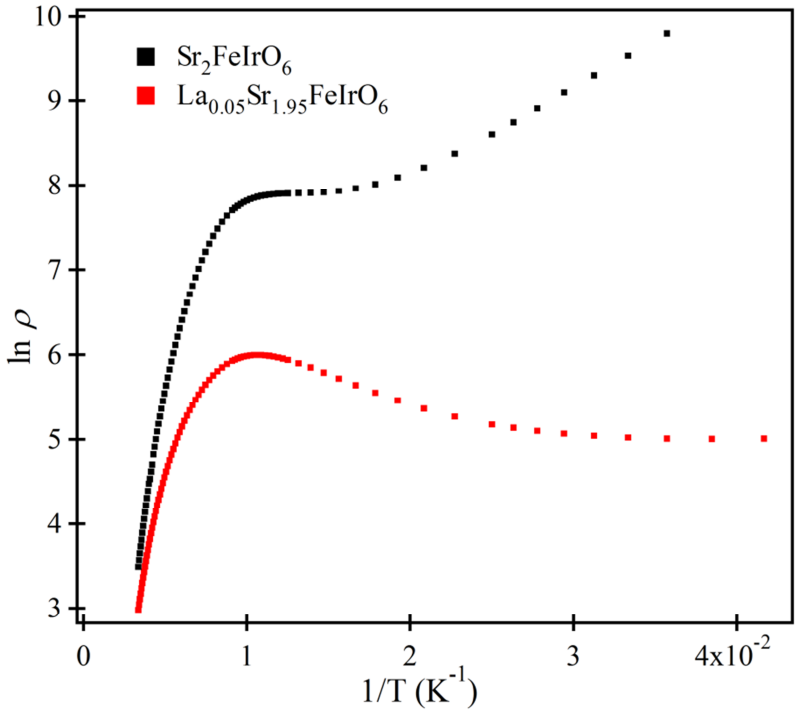

Figure S10. Plot of ln ρ against 1/T for Sr_2FeIrO_6 and $La_{0.05}Sr_{1.95}FeIrO_6$. Linear behavior is not observed over any significant temperature range indicating simple Arrhenius behavior is not followed.

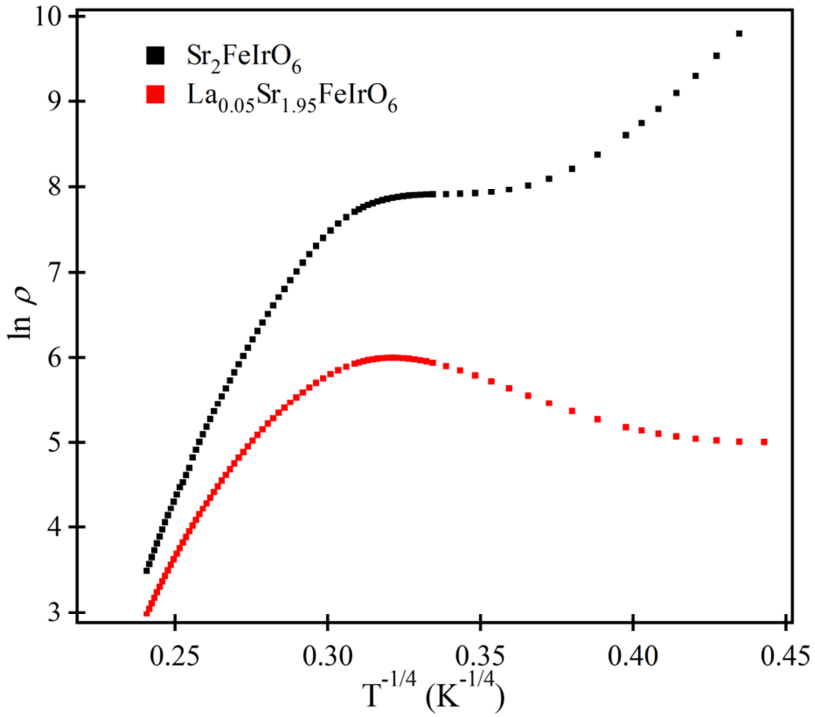

Figure S11. Plot of ln ρ against $T^{-1/4}$ for Sr_2FeIrO_6 and $La_{0.05}Sr_{1.95}FeIrO_6$. Linear behavior is not observed over any significant temperature range indicating variable range hopping behavior is not followed.